

# DIFFRACTIVE MASS SPECTRA AT HERA IN THE INTERACTING GLUON MODEL

F.O. Durães<sup>1\*</sup>, F.S. Navarra<sup>1†</sup> and G. Wilk<sup>1,2‡</sup>

<sup>1</sup>*Instituto de Física, Universidade de São Paulo*

*C.P. 66318, 05315-970 São Paulo, SP, Brazil*

<sup>2</sup>*Soltan Institute for Nuclear Studies, Nuclear Theory Department*

*ul. Hoża 69, 00-681 Warsaw, Poland*

December 28, 2017

## Abstract

We have successfully applied the Interacting Gluon Model (IGM) to calculate diffractive mass spectra measured recently in e-p collisions at HERA. We show that it is possible to treat them in terms of gluon-gluon collisions in the same way as was done before for hadronic collisions. Analysis of available data is performed.

PACS number(s): 13.85.Qk, 11.55.Jy

## 1 Introduction

Diffractive scattering processes are related to the large rapidity gap physics usually interpreted in terms of Pomeron exchange [1]. In hadronic diffractive scattering, one of the incoming hadrons emerges from the collision only slightly deflected and there is a large rapidity gap between it and the other final state particles resulting from the other excited hadron. In the standard Regge theory diffraction is visualised as due to the Pomeron exchange which implies that the excited mass spectrum behaves like  $1/M_X^2$  and does not depend on the energy [2]. The same phenomena can, however, be understood without mentioning

---

\*e-mail: dunga@uspif.if.usp.br

†e-mail: navarra@uspif.if.usp.br

‡e-mail: wilk@fuw.edu.pl

the name of Pomeron by treating  $\mathbb{P}$  as a *preformed colour singlet* object consisting of only a part of the gluonic content of the diffractive projectile which is then absorbed by the other hadron [3]. One possible realization of this idea was developed recently by us [4] (for earlier similar attempts see [5]).

The first test of a theory (or a model) of diffractive dissociation (DD) is the ability to properly describe the mass ( $M_X$ ) distribution of diffractive systems, which has been measured in many hadronic collision experiments [6] and parametrized as  $(M_X^2)^{-\alpha}$  with  $\alpha \simeq 1$ .

Very recently diffractive mass spectra have been measured also in photoproduction processes at high energies at HERA [7]. They were interpreted there in terms of standard Regge theory. In this work we would like to analyse these data using instead the Interacting Gluon Model (IGM) which was already successfully used to describe diffractive mass spectra and their energy dependences in hadronic reactions [4]. The advantage of such approach is the possibility to check what part of the results is due to the simple implementation of conservation laws (notice that IGM was designed in such a way that the energy-momentum conservation is taken care of before all other dynamical aspects - a feature very appropriate for the study of all kinds of energy flows). It means that all notions to the Pomeron (or  $\mathbb{P}$ ) in what follows is just symbolic representation of the DD process.

## 2 IGM picture of a diffractive event

As mentioned in [7], at the HERA electron-proton collider the bulk of the cross section corresponds to photoproduction, in which a beam electron is scattered through a very small angle and a quasi-real photon interacts with the proton. For such small virtualities the dominant interaction mechanism takes place via fluctuation of the photon into a hadronic state which interacts with the proton via the strong force. High energy photoproduction therefore exhibits similar characteristics to hadron-hadron interactions.

In Fig. 1 we show schematically the IGM picture of a diffractive event in a photon-proton collision. According to it, during the interaction the photon is converted into a hadronic (mesonic) state and then interacts with the incoming proton [8]. The meson-proton interaction follows then the usual IGM picture, namely: the valence quarks fly through essentially undisturbed whereas the gluonic clouds of both projectiles interact strongly with each other (by gluonic clouds we understand a sort of "effective gluons" which include also their fluctuations seen as  $\bar{q}q$  sea pairs). The meson loses fraction  $x$  of its original momentum and gets excited forming what we call a *leading jet* (LJ) carrying  $x_L = 1 - x$  fraction of the initial momentum. The proton, which we shall call here the diffracted proton, loses only a fraction  $y$  of its momentum but otherwise remains intact [9].

In the limit  $y \rightarrow 1$ , the whole available energy is stored in  $M_X$  which then remains at rest, i.e.,  $Y_X = 0$ . For small values of  $y$  we have small masses  $M_X$  located at large rapidities  $Y_X$ . In order to regard our process as being truly of the DD type we must assume that all gluons from the target proton participating in the collision (i.e., those emitted from the lower vertex in Fig. 1) have to form a colour singlet. Only then a large rapidity gap will form separating the diffracted proton (in the lower part of our Fig. 1) and the  $M_X$  system (in its upper part), which is the experimental requirement defining a diffractive event. Otherwise a colour string would develop, connecting the diffracted proton and the diffractive cluster, and would eventually decay, filling the rapidity gap with produced secondaries. In this way we are effectively

introducing an object resembling closely to what is known as Pomeron ( $\mathbb{P}$ ) and therefore in what follows we shall use this notion. The Pomeron may be treated [11] as being composed of partons, i.e., gluons and sea  $\bar{q}q$  pairs, in much the same way as hadrons, with some characteristic distribution functions which have been object of studies in HERA experiments [12, 13].

As usual in the IGM [4] we first start with the function  $\chi(x, y)$  describing the probability to form a central gluonic fireball (CF) carrying momentum fractions  $x$  and  $y$  of the two colliding projectiles:

$$\chi(x, y) = \frac{\chi_0}{2\pi\sqrt{D_{xy}}} \cdot \exp \left\{ -\frac{1}{2D_{xy}} [\langle y^2 \rangle (x - \langle x \rangle)^2 + \langle x^2 \rangle (y - \langle y \rangle)^2 - 2\langle xy \rangle (x - \langle x \rangle)(y - \langle y \rangle)] \right\}. \quad (1)$$

For our specific needs in this paper (application to DD events) where we are mostly interested in the  $x$  and  $M_X^2$  behaviour of the results, it is useful to present (1) in the form where the  $x$ -dependence is factorized out:

$$\chi(x, y) = \frac{\chi_0}{2\pi\sqrt{D_{xy}}} \cdot \exp \left[ -\frac{(y - \langle y \rangle)^2}{2\langle y^2 \rangle} \right] \cdot \exp \left\{ -\frac{\langle y^2 \rangle}{2D_{xy}} \left[ x - \langle x \rangle - \frac{\langle xy \rangle}{\langle y^2 \rangle} (y - \langle y \rangle) \right]^2 \right\}. \quad (2)$$

In the above equations

$$D_{xy} = \langle x^2 \rangle \langle y^2 \rangle - \langle xy \rangle^2 \quad (3)$$

and

$$\langle x^n y^m \rangle = \int_0^1 dx x^n \int_0^{y_{max}} dy y^m \omega(x, y). \quad (4)$$

Here  $\chi_0$  denotes the normalization factor provided by the requirement that  $\int_0^1 dx \int_0^1 dy \chi(x, y) \theta(xy - K_{min}^2) = 1$  with  $K_{min} = \frac{m_0}{\sqrt{s}}$  being the minimal inelasticity defined by the mass  $m_0$  of the lightest possible CF and  $\sqrt{s}$  is proton-hadron center of mass energy. In the above expression  $y_{max} = \frac{M_X^2}{s}$ . This upper cut-off, not present in the non-diffractive formulation of the IGM (where  $y_{max} = 1$ ), is necessary to adapt the standard IGM to DD collisions. It is a kinematical restriction preventing the gluons coming from the diffracted proton (and forming our object  $\mathbb{P}$ ) to carry more energy than what is released in the diffractive system. As it will be seen below, it plays a central role in the adaptation of the IGM to DD processes being responsible for its proper  $M_X^2$  dependence. The, so called, spectral function  $\omega(x, y)$  contains all the dynamical inputs of the IGM in the general form given by (cf. [10])

$$\omega(x, y) = \frac{\sigma_{gg}(xys)}{\sigma(s)} G(x) G(y) \Theta(xy - K_{min}^2), \quad (5)$$

where  $G$ 's denote the effective number of gluons from the corresponding projectiles (approximated by the respective gluonic structure functions) and  $\sigma_{gg}$  and  $\sigma$  are the gluonic and hadronic cross sections, respectively. In order to be more precise, the function  $G(y)$ , as it can be seen in Fig. 1, represents the momentum distribution of the gluons belonging to the proton subset called Pomeron and  $y$  is the momentum fraction *of the proton* carried by one of these gluons. We shall therefore use the notation  $G(y) = G_{\mathbb{P}}(y)$ . This function should not be confused with the momentum distribution of the gluons inside the Pomeron,  $f_{g/\mathbb{P}}(\beta)$  (see below).

The moments  $\langle q^n \rangle$ ,  $q = x, y$  (we only require  $n = 1, 2$ ) are given by (4) and are the only places where dynamical quantities like the gluonic and hadronic cross sections appear in the IGM. At this point we emphasize that we are all the time dealing with a meson (essentially the  $\rho^0$ )-proton scattering. However, as was said above, we are in fact selecting a special class of events and therefore we must choose the correct dynamical inputs in the present situation, namely  $G_{\mathbb{P}}(y)$  and the hadronic cross section  $\sigma$  appearing in  $\omega$ .

As pointed out in the introduction, the Pomeron for us is just a collection of gluons which belong to the diffracted proton. In our previous work we have assumed that these gluons behave like all other ordinary gluons in the proton and have therefore the same momentum distribution. The only difference is the momentum sum rule, which for the gluons in  $\mathbb{P}$  is

$$\int_0^1 dy y G_{\mathbb{P}}(y) = p \quad (6)$$

where  $p \simeq 0.05$  (see [4] and below) instead of  $p \simeq 0.5$ , which holds for the entire gluon population in the proton. Alternatively we may treat the Pomeron structure in more detail and address the question of its “hardness” or “softness”. In order to make contact with the analysis performed by HERA experimental groups we consider two possible momentum distributions for the gluons inside  $\mathbb{P}$ :

$$f_{g/\mathbb{P}}^h(\beta) = 6(1 - \beta) \quad (7)$$

and

$$f_{g/\mathbb{P}}^s(\beta) = 6 \frac{(1 - \beta)^5}{\beta} \quad (8)$$

where  $\beta$  is the momentum fraction of the Pomeron carried by the gluons and the superscripts  $h$  and  $s$  denote hard and soft respectively. We follow here the (standard) notation of ref. [12]. We shall use the Pomeron flux factor given by

$$f_{\mathbb{P}/p}(x_{\mathbb{P}}) = \frac{1}{x_{\mathbb{P}}} \quad (9)$$

where  $x_{\mathbb{P}}$  is the fraction of the proton momentum carried by the Pomeron and the normalization will be fixed later. Noticing that  $\beta = \frac{x}{x_{\mathbb{P}}}$  the distribution  $G_{\mathbb{P}}(y)$  needed in eq. (5) is then given by the convolution:

$$G_{\mathbb{P}}^{h,s}(y) = \int_y^1 \frac{dx_{\mathbb{P}}}{x_{\mathbb{P}}} f_{\mathbb{P}/p}(x_{\mathbb{P}}) f_{g/\mathbb{P}}^{h,s}\left(\frac{y}{x_{\mathbb{P}}}\right) \quad (10)$$

In our calculations we shall also use  $G_{\mathbb{P}}(y) = 6 \frac{(1-y)^5}{y}$ , the same expression already used by us before [4]. As it will be seen this choice corresponds to an intermediate between “soft” and “hard” Pomeron. In the upper leg of Fig. 1 we assume, for simplicity, the vector meson to be  $\rho^0$  and take  $G^{\rho^0}(x) = G^\pi(x)$ . The fraction of diffracted nucleon momentum,  $p$ , allocated specifically to the  $\mathbb{P}$  gluonic cluster and the hadronic cross section  $\sigma$  are both unknown. However, they always appear in  $\omega$  as a ratio ( $\frac{p}{\sigma}$ ) of parameters and different choices are possible. Just in order to make use of the present knowledge about the Pomeron, we shall choose

$$\sigma(s) = \sigma^{\mathbb{P}p} = a + b \ln \frac{s}{s_0} \quad (11)$$

where  $s_0 = 1 \text{ GeV}^2$  and  $a = 2.6 \text{ mb}$  and  $b = 0.01 \text{ mb}$  are parameters fixed from a previous [4] systematic data analysis. As it can be seen,  $\sigma(s)$  turns out to be a very slowly varying function of  $\sqrt{s}$  assuming values between 2.6 and 3.0 mb, which is a well accepted value for the Pomeron-proton cross section, and  $p \simeq 0.05$  (cf. [4]). Since the parameter  $\frac{p}{\sigma}$  has been fixed considering the proton-proton diffractive dissociation and we are now addressing the  $p - \rho^0$  case we have some freedom to change  $\sigma$ . In the following we shall also investigate the effect of small changes in the value of  $m_0$  on our final results.

Although in the final numerical calculations the above complete formulation will be used, it is worthwhile to present approximate analytical results in order to illustrate the main characteristic features of the IGM. It is straightforward to show that, keeping only the most singular terms in gluon distribution functions, i.e.,  $G(x) = G_{\mathbb{P}}^{h,s}(x) \simeq \frac{1}{x}$  and only the leading terms in  $\sqrt{s}$ , one finds that for any choice of  $\sigma_{gg}$  in (5):

(i) terms containing the mixed moment  $\langle xy \rangle$  can be always neglected in comparison to those containing  $\langle x^2 \rangle$  or  $\langle y^2 \rangle$  (i.e., for example,  $D_{xy} \simeq \langle x^2 \rangle \langle y^2 \rangle$ );

(ii) all moments are related in the following way:

$$\langle x^2 \rangle \simeq \frac{1}{2} \langle x \rangle; \quad \langle y \rangle \simeq y_{max} \langle x \rangle; \quad \langle y^2 \rangle \simeq \frac{1}{2} y_{max} \langle y \rangle; \quad (12)$$

i.e., all results can be expressed in terms of the  $\langle x \rangle$  moment only;

(iii) the  $\langle x \rangle$  moment has the following simple behaviour depending on the type of  $\sigma_{gg}$  chosen in (5):

$$\langle x \rangle \simeq const, \quad \simeq \ln \left( \frac{sy_{max}}{m_0^2} \right), \quad \simeq \frac{1}{2} \ln^2 \left( \frac{sy_{max}}{m_0^2} \right) \quad \text{for} \quad \sigma_{gg} \simeq \frac{m_0^2}{xys}, \quad \simeq const, \quad \simeq \ln \left( \frac{xys}{m_0^2} \right), \quad (13)$$

respectively.

This allows us to write eq.(2) in a very simple form:

$$\chi(x, y) \simeq \frac{\chi_0}{\pi y_{max} \langle x \rangle} \cdot \exp \left[ -\frac{(y - y_{max} \langle x \rangle)^2}{y_{max}^2 \langle x \rangle} \right] \cdot \exp \left[ -\frac{(x - \langle x \rangle)^2}{\langle x \rangle} \right]. \quad (14)$$

As already mentioned, the  $\frac{1}{y_{max}}$  term present in (14) can be traced back to the upper cut-off  $y = y_{max}$  in (4) above. Because it is defined by the produced diffractive mass,  $y_{max} = \frac{M_X^2}{s}$ , it provides then automatically the  $\frac{1}{M_X^2}$  behaviour. The other two factors have a much weaker dependence on  $M_X^2$  and they tend to compensate each other (they provide, however, all possible non-trivial energy dependence of DD, cf. [4]).

### 3 Comparison with experimental data

The IGM diffractive mass spectrum is given by [4]:

$$\begin{aligned} \frac{dN}{dM_X^2} &= \int_0^1 dx \int_0^1 dy \chi(x, y) \delta(M_X^2 - sy) \Theta(xy - K_{min}^2) \\ &= \frac{1}{s} \int_{\frac{m_0^2}{M_X^2}}^1 dx \chi \left( x, y = \frac{M_X^2}{s} \right), \end{aligned} \quad (15)$$

or, in the approximate form,

$$\frac{dN}{dM_X^2} \simeq \frac{1}{M_X^2} \cdot \frac{\chi_0}{\pi \langle x \rangle} \exp \left[ -\frac{(1 - \langle x \rangle)^2}{\langle x \rangle} \right] \int_{\frac{m_0^2}{M_X^2}}^1 dx \exp \left[ -\frac{(x - \langle x \rangle)^2}{\langle x \rangle} \right]. \quad (16)$$

We would like to emphasize two aspects of the approximate formula above:

- (i) it explicitly exhibits the characteristic  $M_X^2$  dependence of diffractive collisions, namely it shows the  $(M_X^2)^{-\alpha}$  behaviour with  $\alpha \simeq 1$ ;
- (ii) the exponential and integral factors have a very weak dependence on  $M_X^2$  but they contain a non-trivial energy  $\sqrt{s}$  dependence, which is intrinsic to the model and comes ultimately from phase space limits and cross sections contained in eq.(5).

In Fig. 2 we compare eq.(15) with the recent data from the H1 collaboration [7]. In all formulas  $\sqrt{s}$  will now be replaced by  $W$ , the photon-proton center of mass energy. Figure 2a (2b) presents data for  $W = 187$  GeV ( $W = 231$  GeV). The different curves correspond to the choices I ( $m_0 = 0.31$  GeV,  $\sigma = 2.7$  mb), II ( $m_0 = 0.35$  GeV,  $\sigma = 2.7$  mb), III ( $m_0 = 0.31$  GeV,  $\sigma = 5.4$  mb) and IV ( $m_0 = 0.35$  GeV,  $\sigma = 5.4$  mb), respectively. In all these curves we have used  $G_P(y) = 6 \frac{(1-y)^5}{y}$ . As expected, the distribution at low  $M_X^2$  is very sensitive to threshold effects. When we go from the upper to the lower solid (dashed) lines we can observe that the increase of the Pomeron-hadron cross section changes the distribution in such a way that larger masses  $M_X^2$  are favoured.

We would like to stress that in curve II there is no free or new parameter. All parameter values are the same as in our previous paper devoted to hadronic diffraction. It misses only the very small mass region points, where we expect it to be below the data, since we do not include resonance effects. In the large mass region a better agreement with data may be achieved with a somewhat larger value of the Pomeron-hadron cross section. This region may, however, be influenced by other effects, one of which we discuss below.

In Fig. 3 we compare the same data ( $W = 187$  GeV) with our mass spectrum obtained with  $G_P^h(y)$  (curve I),  $G_P(y)$  (curve II) and  $G_P^s(y)$  (curve III). This comparison suggests that the “hard” Pomeron can give a good description of data. The same can be said about our “mixed” Pomeron, which, in fact seems to be more hard than soft. These three curves were calculated with exactly the same parameters and normalizations, the only difference being the Pomeron profile. Apparently the “soft” Pomeron (curve III) is ruled out by data. Curve IV shows, however, that with a different choice of parameters  $m_0 = 0.50$  GeV and  $\sigma = 5.4$  mb a good agreement is again obtained. Considering the large amount of data already described previously by the IGM, this choice is extreme. We conclude therefore that the “soft” Pomeron is disfavoured. This same conclusion was found in refs. [12, 13].

A very interesting question regarding DD processes is whether or not semihard interactions play a role in diffractive physics. In hadronic non-diffractive collisions semihard scatterings are expected to be visible at c.m.s. energies around  $\sqrt{s} \simeq 500$  GeV. In such scatterings two partons interact with a momentum transfer of  $p_T \simeq 2 - 4$  GeV, forming two so-called minijets. Since  $\Lambda_{QCD} \ll p_T \ll \sqrt{s}$ , minijet cross sections can be calculated with perturbative QCD and they are large enough to be relevant for minimum bias physics. In the IGM, energy deposition is occurring due to gluon-gluon collisions in

both perturbative (semihard) and non-perturbative regimes. The gluon-gluon cross section in eq. (5) is computed with perturbative QCD or with a non-perturbative ansatz according to the scale ( $= xys$ ). The relative importance of minijets with respect to the soft processes was fixed following the experimental estimates of the minijet cross section made by the CERN UA1 and UA5 collaborations in hadronic collisions. We have been assuming so far that the onset of semihard physics in DD occurs at the same energy as in ordinary non-diffractive processes. This may not be true, or even if it is true, there are uncertainties regarding the precise value of the relevant energy scale. In Fig. 4 we repeat the fit of Fig. 2 using only curves II, which are our “conservative” calculation, plotted with solid lines. Since the present energies are not yet very large, we could just neglect the small minijet component. The dashed curves in Fig. 4 show the effect of switching off the semihard contribution. There is only a small enhancement in the tail of the spectra. Without minijets the energy deposition in the central blob of Fig. 1 is decreased and the leading particle, in the upper leg ( $\rho$  meson after interaction), is more energetic. It contributes more to the diffractive mass  $M_X^2$  and makes it larger. This effect is negligible for very low  $M_X^2$  but becomes visible at large diffractive masses. Repeating this comparison (total spectrum versus the spectrum without minijets) at higher energies we observe that the magnitude of the minijet contribution is always small and shows always the tendency to produce slightly faster falling distributions at the end of the spectrum. This suggests that in DD processes minijets are unimportant even at very high energies.

## 4 Summary and conclusions

In conclusion, a straightforward (and with no new parameter) extension of our model of hadronic diffraction to photon-proton reactions is able to fit the data for diffractive mass excitation presented in ref. [7] within small discrepancies. The agreement may become better with some small changes motivated by uncertainties in previous fitting procedures.

Our analysis of data suggests that the Pomeron is “hard” and undergoes mostly “soft” interactions. This means that this object is composed by a relatively “small” number of gluons carrying each, in the average a large fraction of the Pomeron momentum, but a small fraction of the total momentum of the proton and undergoing mostly soft (with respect to a hard energy scale  $\simeq 2 - 3$  GeV) collisions with the gluons of the other hadron.

The fact that our model is successful means that energy flow in many and different high energy reactions can be understood as an incoherent superposition of parton-parton scatterings constrained by energy conservation.

Acknowledgements: This work has been supported by FAPESP, CNPQ (Brazil) and KBN (Poland). We would like to warmly thank R. Covolan and E. Ferreira for many fruitful discussions. GW would also like to thank IFUSP for warm hospitality extended to him during his visit there.

## References

- [1] J.D.Bjorken, *Nucl. Phys. (Proc. Suppl.)* **B25** (1992) 253.

- [2] K.Goulianos, *Phys. Rep.* **101** (1983) 169.
- [3] A.Edin, G.Ingelman and J.Rathsman, *Phys. Lett.* **B366** (1996) 371 and references therein.
- [4] F.O.Durães, F.S.Navarra and G.Wilk, *Phys. Rev.* **D55** (1997) 2708 and references therein.
- [5] B.R.Desai and U.P.Sukhatme, *Z. Phys.* **C24** (1984) 277; V.Innocente et al., *Phys. Lett.* **B169** (1986) 285; L.Lönnblad, *Z. Phys.* **C65** (1995) 285; J.C.Collins et al., *Phys. Rev.* **D51** (1995) 3182.
- [6] N.A.Amos et al. (E710 Collab.), *Phys. Lett.* **B301** (1993) 313; F.Abe et al. (CDF Collab.), *Phys. Rev.* **D50** (1994) 5535 (and references therein). Cf. also M.Bozzo et al. (UA4 Collab.), *Phys. Lett.* **B136** (1984) 217.
- [7] H1 Collaboration: C. Adloff et al., *Z. Phys.* **C74** (1997) 221.
- [8] J.Sakurai, *Ann. Phys.* **11** (1960) 1 and *Phys. Rev. Lett.* (1969) 981.
- [9] It can be also deflected with some invariant momentum transfer  $t$ . However, because the IGM does not include so far any transverse momentum transfers, the results presented here must be regarded as appropriately averaged/integrated over  $t$ .
- [10] F.O.Durães, F.S.Navarra and G.Wilk, *Phys. Rev.* **D47** (1993) 3049.
- [11] G.Ingelman and P.Schlein, *Phys. Lett.* **B152** (1985) 256; A.Donnachie and P.V.Landshoff, *Phys. Lett.* **B191** (1987) 309; *Nucl. Phys.* **B303** (1988) 634.
- [12] ZEUS Collaboration: M.Derrick et al., *Phys. Lett.* **B356** (1995) 129; *Z. Phys.* **C68** (1995) 569 and references therein.
- [13] H1 Collaboration: T. Ahmed et al., *Nucl. Phys.* **B435** (1995) 3; **B429** (1994) 477.

## Figure Captions

**Fig. 1** IGM description of a photon-proton scattering with the formation of a diffractive system of invariant mass  $M_X$ .

**Fig. 2a** Diffractive mass spectrum for  $\gamma p$  collisions at  $W = 187$  GeV calculated with the IGM (eq.(15)) and compared with H1 data [7]. The different curves correspond to the choices: I ( $m_0 = 0.31$  GeV,  $\sigma = 2.7$  mb), II ( $m_0 = 0.35$  GeV,  $\sigma = 2.7$  mb), III ( $m_0 = 0.31$  GeV,  $\sigma = 5.4$  mb) and IV ( $m_0 = 0.35$  GeV,  $\sigma = 5.4$  mb), respectively.

**Fig. 2b** The same as Fig. 2a for  $W = 231$  GeV.

**Fig. 3** Data from ref. [7] compared with eq. (15). The solid line (curve II) corresponds to the choice  $m_0 = 0.35$  GeV,  $\sigma = 2.7$  mb and  $G_P(y)$ . Curves I (dashed) and III (dotted) are obtained replacing  $G_P(y)$  by  $G_P^h(y)$  and  $G_P^s(y)$  respectively. Curve IV is obtained with  $G_P^s(y)$  and  $m_0 = 0.50$  GeV and  $\sigma = 5.4$  mb.



**Fig. 4a** Diffractive mass spectrum for  $\gamma p$  collisions at  $W = 187$  GeV, curve II of Fig. 2a, shown with a solid line and compared with the same spectrum without the minijet contribution (dashed line).

**Fig. 4b** The same as Fig. 3a for  $W = 231$  GeV.

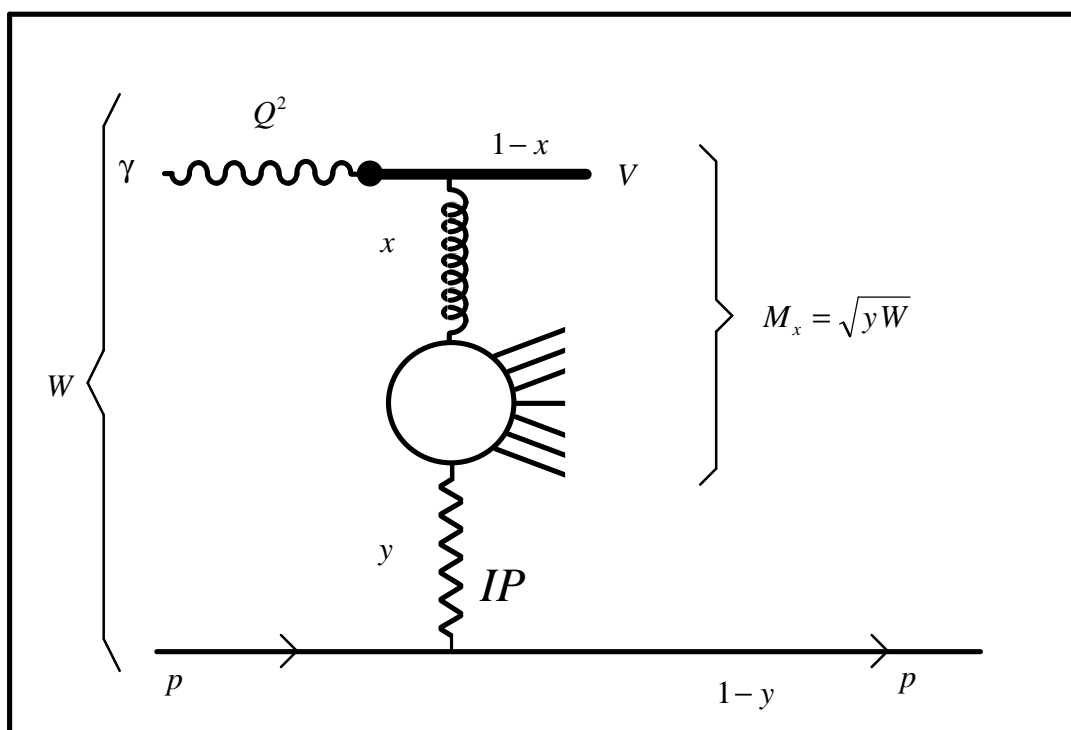
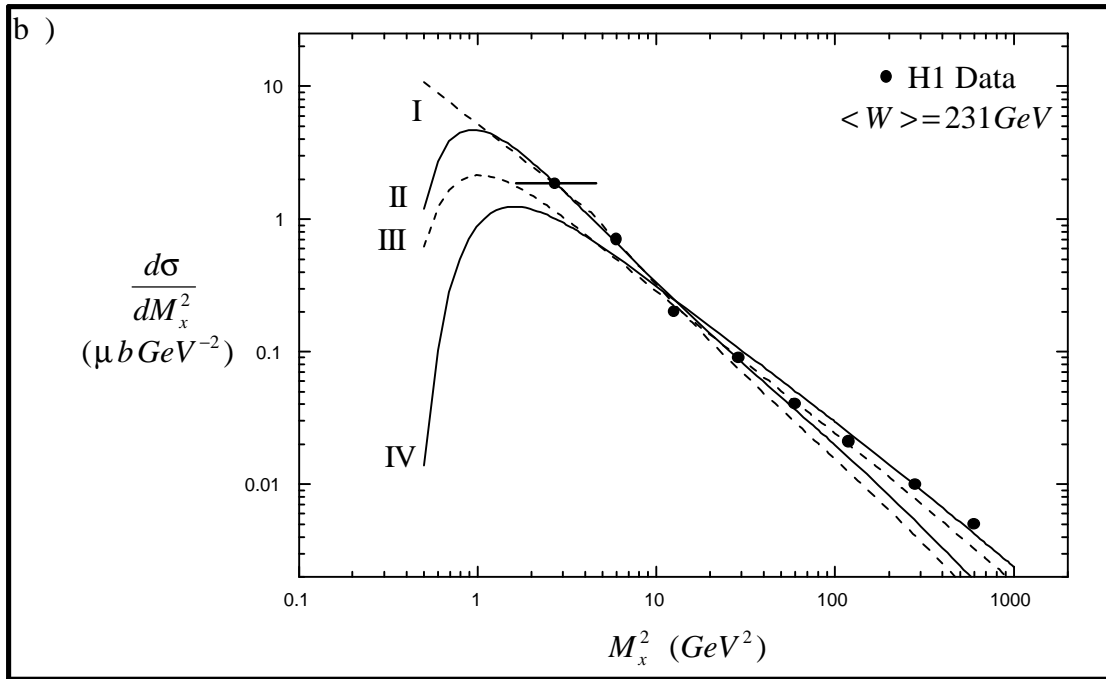
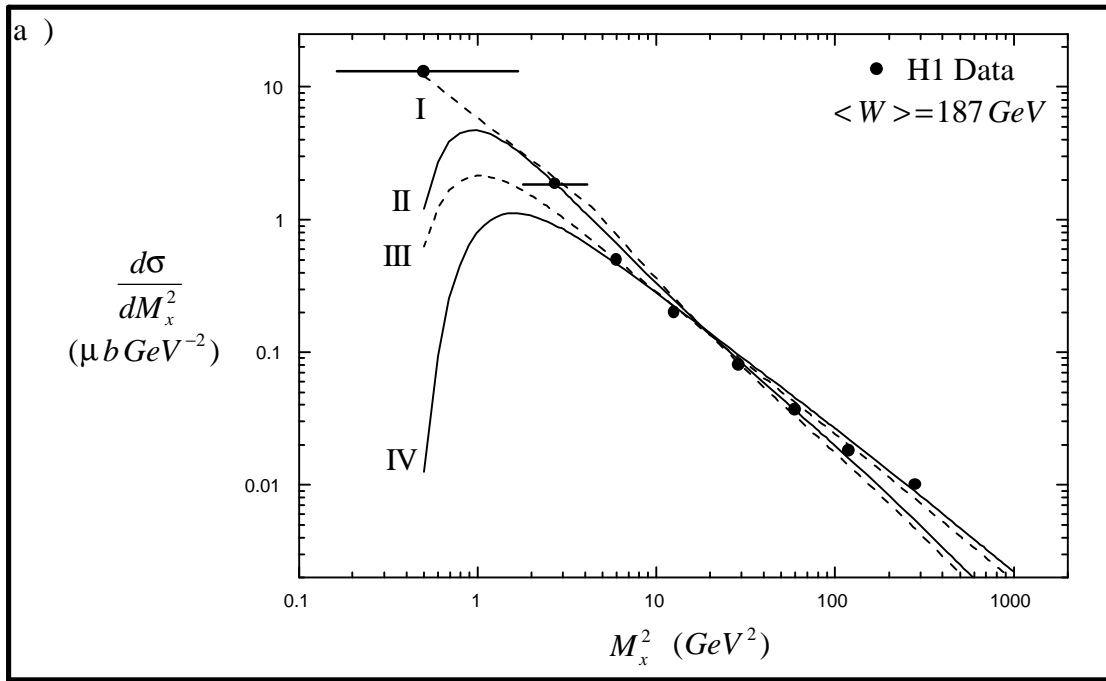


Figure 1



**Figure 2**

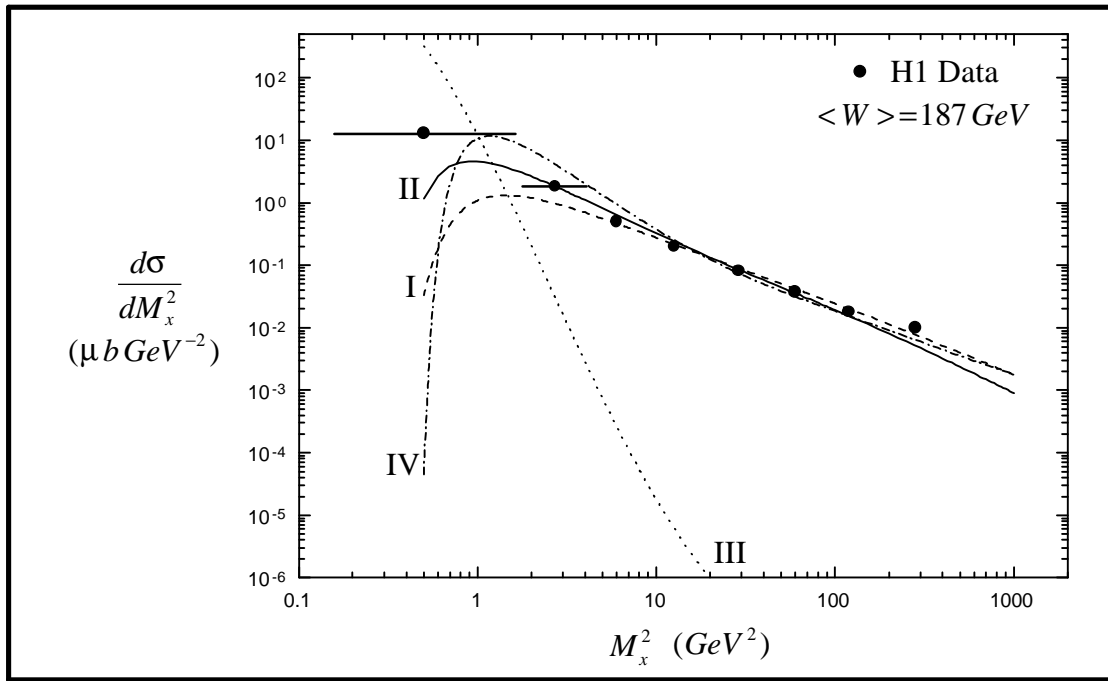


Figure 3

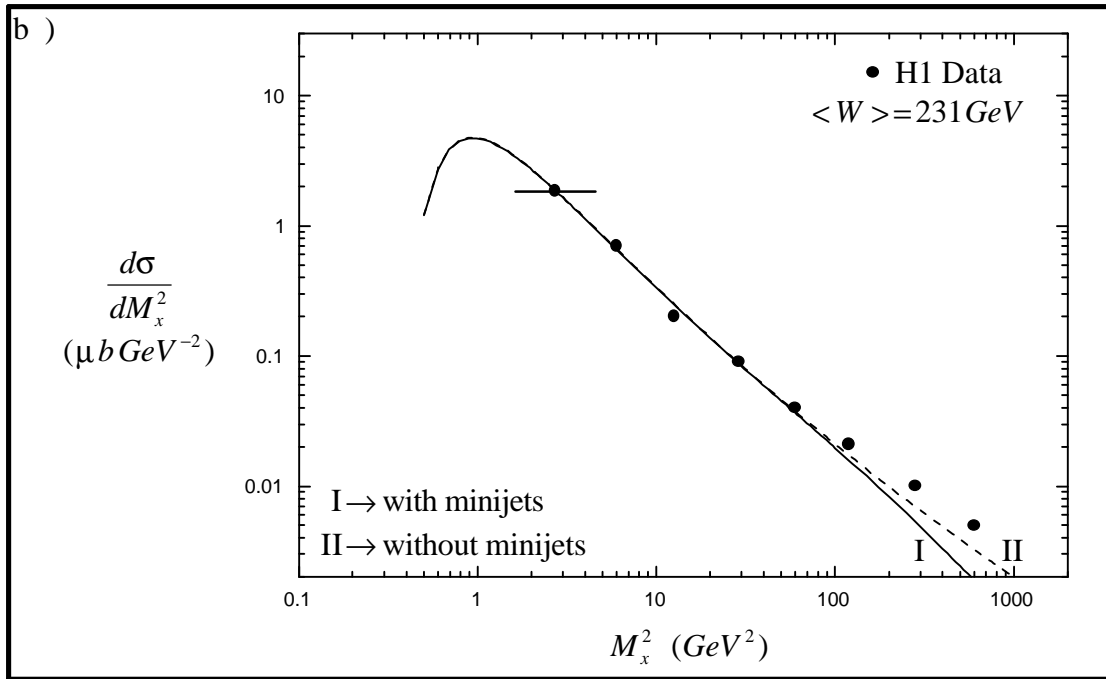
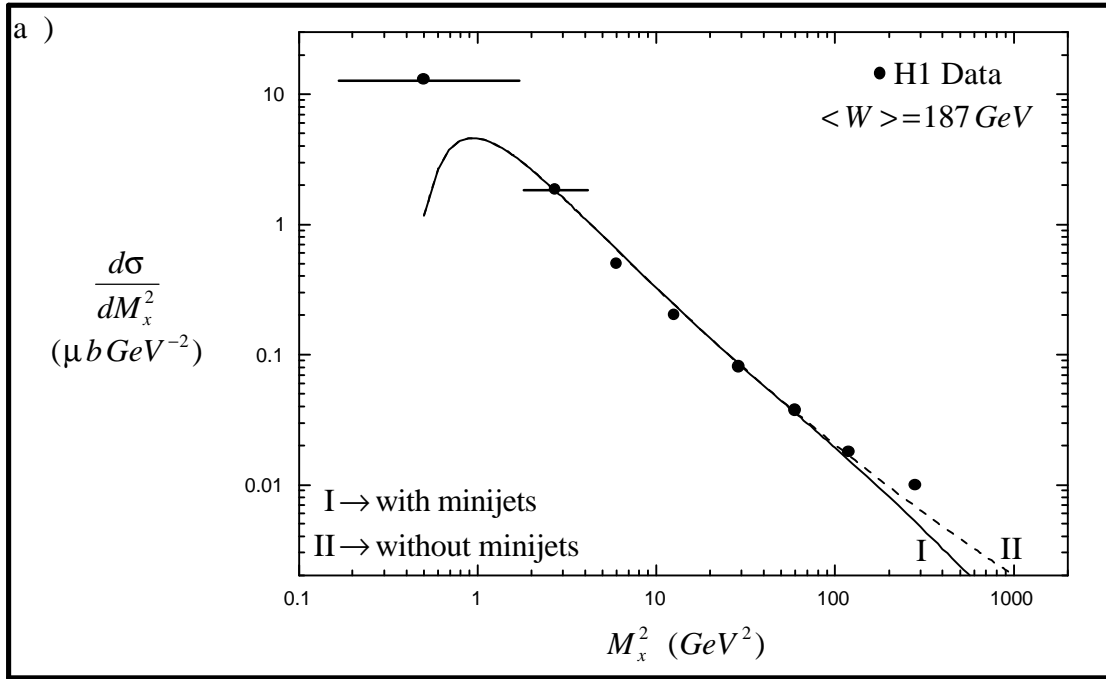


Figure 4